2012

Effect of Microfins on Heat Rejection in Desuperheating, Condensation in Superheated Region and Two Phase Zone

Predrag S. Hrnjak
pega@illinois.edu

Chieko Kondo

Effect of Microfins on Heat Rejection in Desuperheating, Condensation in Superheated Region and Two Phase Zone

Pega HRNJAK[1]*, Chieko KONDOU[2]

[1]University of Illinois, Mechanical Science and Engineering ACRC, West Green, Urbana, IL 61801, USA
also Creative Thermal Solutions, Inc., 2209 North Willow Road, Urbana, IL 61802, USA
Phone: +1 (217) 244-6377, E-mail: pega@illinois.edu

[2]Kyushu University, Interdisciplinary Graduate School of Engineering Science,
6-1, Kasuga, Fukuoka, 816-8580 Japan
Phone: +81 (92) 583-7832, E-mail: kondo.chieko.162@m.kyushu-u.ac.jp

ABSTRACT

Typical condenser design model simply divides the heat rejection process into de-superheating, two-phase, and subcooling. By neglecting condensation in presence of superheated vapor, error can be introduced. Experimental data on superheated CO_2 and R410A flow in horizontal microfin tubes of 6 mm inner diameter at reduced pressures from 0.55 to 0.95 are provided. Gradually increasing heat transfer coefficient, from when tube wall reaches saturation temperature, demonstrates the criteria of condensation occurrence and the proposed heat transfer model.

1. INTRODUCTION

When heat rejection is close to critical point in subcritical cycles, the degree of superheat at compressor discharge is much higher than in conventional cycles operating at low reduced pressure mostly because the latent heat becomes smaller. Therefore, the portion of superheat zone (i.e., de-superheating zone) in the heat rejection exchanger is necessary to be considered for proper sizing and circuit designing of condensers. Typical calculation models divide the heat rejection process three zones: de-superheating, condensation and subcooling, even it is clear that condensation occurs in de-superheating zone at some conditions and that subcooling occurs during condensation. Of primary concern in this study is actual situation of subcritical heat rejection process in helical microfin tubes, which are widely used in condensers of air conditioner and refrigeration systems.

Altman et al. (1959) provided six points of experimentally determined heat transfer coefficient (HTC), which are averaged from various superheated inlet to saturated outlet in a test section of 1.22 m length and 8.71 mm inner diameter (ID). With various degrees of inlet superheat, approximately 30 to 70 % of decrease in HTC from a correlation valid for saturated condensation was confirmed. Bell (1972) proposed the criterion of condensation occurrence in de-superheating zone, which is tube wall temperature below saturation point, and cautioned that the simple use of LMTD (logarithmic mean temperature difference) method to calculate the overall coefficient of condensers could be invalid. Fujii et al. (1978) experimentally investigated condensation of R11 and R113 flow in horizontal smooth tubes. From the measured temperature distribution in the radial direction of the horizontal middle plane of the tube, coexistence of superheated vapor and subcooled liquid in condensation flow was demonstrated. By using the vapor mass quality, which indicates actual vapor and liquid mass flow rate in non-equilibrium, the mass transport process from superheated vapor was analyzed. Lee et al. (1991) experimentally investigated condensation in superheated R22 vapor and proposed a physical model taking account of the sensible heat rejected from superheated vapor into overall condensation heat transfer. In response, Webb (1998) reported that the sensible heat is negligible and a simplified model defines HTC with saturation temperature gives same results to Lee's model. A number of data was provided by Kedzierski and Goncalves (1997) includes some experimental HTC of superheated R125, R134a, R32, and R410 vapor in helical microfin tubes. Their R410A HTC appears to be gradually increasing from superheat zone to two-phase zone; however, the data was not sufficient for qualitative assessment of it. Later, in the experimental results by Kondou and Hrnjak (2012), this gradual transition from superheat to two-phase zone was quantified for subcritical CO_2 and R410A condensation in smooth tubes. This paper provides the experimental HTC of subcritical condensation from superheated CO_2 and R410A flow in helical microfin tubes to validate the heat transfer model of condensing superheat zone at more practical conditions.

2. HEAT TRANSFER MODEL FOR CONDENSING IN SUPERHEAT ZONE

Figure 1 illustrates heat rejection process in one circuit of a condenser. Superheated vapor rejects heat in sensible way along a single-phase superheat zone. At a certain point, being exposed to tube wall at temperature below saturation, superheated vapor starts condensing. From that point on, condensate is present and actual vapor quality x_a of non-equilibrium state is below 1, while thermodynamic vapor quality (or equilibrium vapor quality) x_b is still beyond 1. Then, saturated condensation occurs from thermodynamic vapor quality 1, where the bulk temperature is nearly equal to the saturation temperature. Saturated refrigerant mostly rejects latent heat during condensation and minute of sensible heat from subcooled condensate.

Figure 2 explains heat balance in a short cooling segment of the condensing superheat zone ($1 < x_b$, $x_a < 1$). From the continuity, the total mass flow rate of vapor and liquid refrigerant $\dot{m}_{total}$ is,

$$\dot{m}_{total} = \dot{m}_{V,i} + \dot{m}_{L,i} = \dot{m}_{V,o} + \dot{m}_{L,o} \tag{1}$$

The amount of condensate generated through a segment $\Delta\dot{m}_L$ is expressed from the continuity as,

$$\Delta\dot{m}_L = \dot{m}_{L,o} - \dot{m}_{L,i} = \dot{m}_{V,i} - \dot{m}_{V,o} = \Delta\dot{m}_V \tag{2}$$

The average specific enthalpies in superheated vapor and subcooled liquid are represented with their specific heat: Cp_V and Cp_L, and degree of superheat and subcool: ΔT_{SH} and ΔT_{SC}.

$$\left.\begin{aligned} \overline{h}_V &= h_{Vsat} + \overline{Cp_V \Delta T_{SH}} = h_{Vsat} + \overline{\Delta h_{SH}} \\ \overline{h}_L &= h_{Lsat} - \overline{Cp_L \Delta T_{SC}} = h_{Vsat} - \Delta h_{LV} - \overline{\Delta h_{SC}} \end{aligned}\right\} \tag{3}$$

Difference of total enthalpy from inlet to outlet is the rejected heat from a segment.

$$h_{b,i}\dot{m}_{total} = \overline{h}_{V,i}\dot{m}_{V,i} + \overline{h}_{L,i}\dot{m}_{L,i} = \left(h_{Vsat} + \overline{\Delta h_{SH,i}}\right)\dot{m}_{V,i} + \left(h_{Vsat} - \Delta h_{LV} - \overline{\Delta h_{SC,i}}\right)\dot{m}_{L,i} \tag{4}$$

$$h_{b,o}\dot{m}_{total} = \overline{h}_{V,o}\dot{m}_{V,o} + \overline{h}_{L,o}\dot{m}_{L,o} = \left(h_{Vsat} + \overline{\Delta h_{SH,o}}\right)\left(\dot{m}_{V,i} - \Delta\dot{m}_L\right) + \left(h_{Vsat} - \Delta h_{LV} - \overline{\Delta h_{SC,o}}\right)\left(\dot{m}_{L,i} + \Delta\dot{m}_L\right) \tag{5}$$

$$\left(h_{b,i} - h_{b,o}\right)\dot{m}_{total} = \underbrace{\left(\overline{\Delta h_{SH,i}} - \overline{\Delta h_{SH,o}}\right)\dot{m}_{V,i} + \overline{\Delta h_{SH,o}}\Delta\dot{m}_L}_{SH} + \underbrace{\Delta h_{LV}\Delta\dot{m}}_{latent} + \underbrace{\left(\overline{\Delta h_{SC,o}} - \overline{\Delta h_{SC,i}}\right)\dot{m}_{L,i} + \Delta h_{SC,o}\Delta\dot{m}_L}_{SC} \tag{6}$$

As divided into three terms in Equation (6), the heat rejection of condensing superheat zone is caused by de-superheating of vapor flow, latent heat rejection to generate condensate, and subcooling of condensate. When those three sorts of heat pass though the same heat transfer area of interior tube wall, the heat flux can be expressed as,

$$q_{total} = q_{SH} + \left(q_{latent} + q_{SC}\right) \tag{8}$$

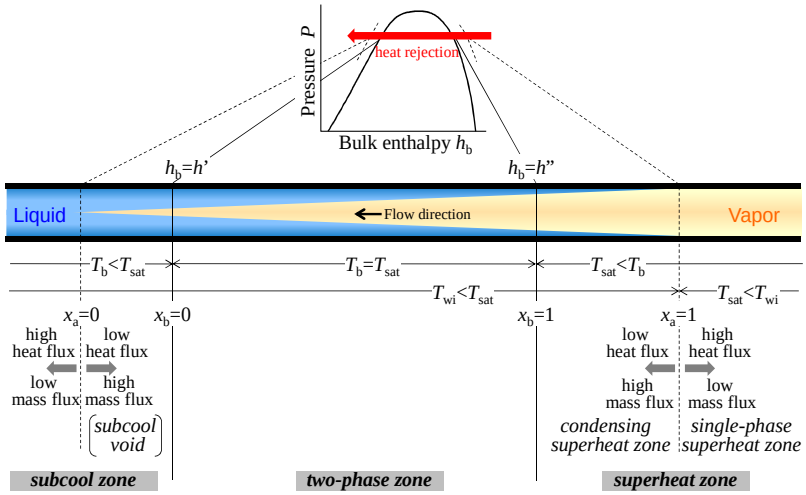

Figure 1: Heat rejection process in condensers

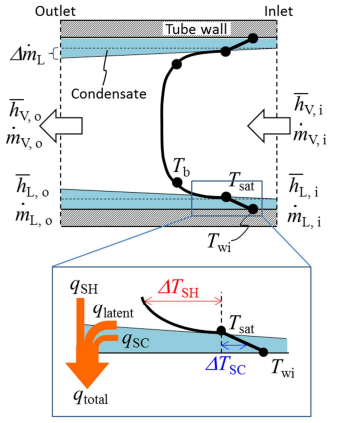

Figure 2: Heat balance in condensing superheat zone

The driving temperature difference of the de-superheating heat flux q_{SH} is nearly "bulk-to-saturation" (T_b - T_{sat}). The remaining heat flux (q_{latent} + q_{SC}) can be manipulated as saturated condensation, because condensation postulates degree of subcool on cooling surface. That driving temperature difference is normally taken as "saturation-to-wall" (T_{sat} - T_{wi}). Hence, overall HTC base on the interior tube wall is,

$$\alpha \approx \alpha_{SH}\left(\frac{T_b - T_{sat}}{T_b - T_{wi}}\right) + \alpha_{TP}\left(\frac{T_{sat} - T_{wi}}{T_b - T_{wi}}\right) \tag{9}$$

3. EXPERIMENTAL SETUP AND METHOD

3.1 Test Section and Test Tube

Figure 3 (a) shows arrangement and structure of a test section. The test section is located after a pre-heater, a mixer, and a pre-cooler. By the electric pre-heater, superheat is kept from 5 to 50 K. In the mixer, pressure and bulk-mean-temperature of superheated refrigerant flow is measured for finding the specific enthalpy. In the pre-cooler, superheat and enthalpy at the test section inlet is precisely adjusted by controlling the temperature and flow rate of cooling water. While the superheat is adjusted above 5 K for making a condition of superheat zone, the cooling water is shut. In the test section, a test tube is placed horizontally and covered with a thick brass jacket having water channels for adjusting the average heat flux under uniform temperature cooling. The active cooling length by the brass jacket is 150 mm, which is relatively short for measuring quasi-local HTC in axial direction. Figure 3 (b) shows the cross section of the test tube is layered by outer tube, solder alloy, and test microfin tube. Twelve thermocouples are embedded in the solder layer, on the top, bottom, right, and left of the test microfin tube outer surface at three positions in the axial direction. The dimensions of those microfin tubes A and B having helical microfins internally and a comparative smooth tube are specified in Table 1.

3.2 Data Reduction Procedure

From the pressure and bulk mean temperature measured in the mixer, the enthalpy of superheated vapor refrigerant is determined by an equilibrium state equation of REFPROP ver.8 (Lemmon *et al*., 2008). The enthalpy changes in the pre-cooler and the test section are found from the heat balance of cooling water; meanwhile, the pressure drops through the pre-cooler and the test section are measured. Then, the test section inlet, outlet, and the center refrigerant temperature: $T_{b,i}$, $T_{b,o}$, and T_b, are found from those enthalpies and pressures.

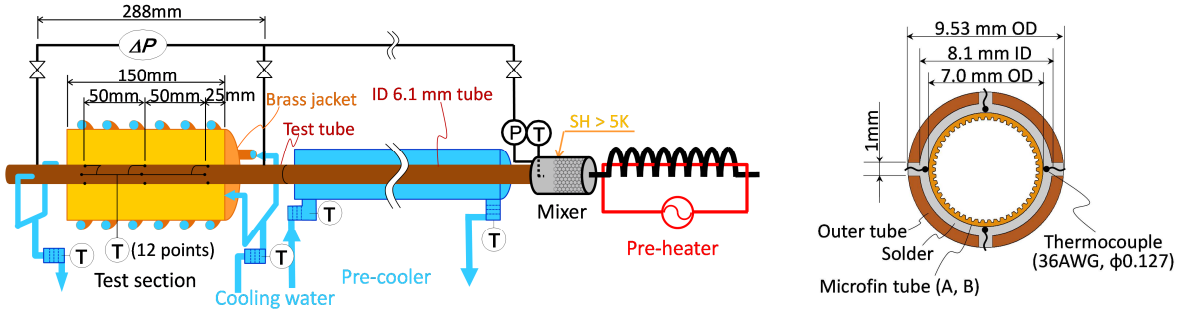

(a) test section arrangement (partially halved for showing internal structure) (b) test tube

Figure 3: Structure of the test section and the test tube

Table 1: Dimensions of the test microfin tubes

			Smooth	Microfin A	Microfin B	Nomenclatures of fin geometries
Equivalent inner diameter*	d_{eq}	[mm]	6.10	6.35	6.14	(Cross section of microfin tubes)
Nominal inner diameter	d_{max}	[mm]	6.10	6.50	6.50	
Fin height	d_{fin}	[mm]	-	0.18	0.24	
Number of fins	N_{fin}	[-]	-	50	55	
Lead angle	β	[°]	-	18	27	
Apex angle	γ	[°]	-	42	15	
Surface enlargement**	η_A	[%]	-	172	207	

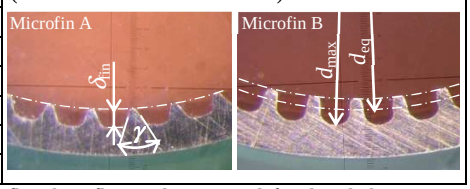

*Inner diameter of the smooth tube having same cross sectional free flow area. Mass flux, heat flux, and HTC are defined at d_{eq} but not d_{max} nor enlarged surface. ** Compared to the equivalent smooth tube.

$$\left.\begin{aligned} T_{\mathrm{b,i}} &= f_{equiblium,\,REFPROP8}\left(h_{\mathrm{b,Mixer}} - \Delta h_{\mathrm{PC}}, P_{\mathrm{Mixer}} - \Delta P_{\mathrm{PC}}\right) \\ T_{\mathrm{b,o}} &= f_{equiblium,\,REFPROP8}\left(h_{\mathrm{b,Mxer}} - \Delta h_{\mathrm{PC}} - \Delta h_{\mathrm{TS}}, P_{\mathrm{Mixer}} - \Delta P_{\mathrm{PC}} - \Delta P_{\mathrm{TS}}\right) \\ T_{\mathrm{b}} &= \left(T_{\mathrm{b,i}} + T_{\mathrm{b,o}}\right)/2 \end{aligned}\right\} \quad (10)$$

The heat flux $q_{\mathrm{wi,\,eq}}$ is defined on the interior surface of the equivalent smooth tube as,

$$q_{\mathrm{wi,\,eq}} = Q_{\mathrm{TS}}/\left(d_{\mathrm{eq}}\cdot\pi\cdot\Delta Z_{\alpha}\right) = \left(Q_{\mathrm{H2O,TS}} - Q_{\mathrm{gain,TS}} - Q_{\mathrm{cond}}\right)/\left(d_{\mathrm{eq}}\cdot\pi\cdot\Delta Z_{\alpha}\right) \quad (11)$$

where, d_{eq} and ΔZ_{α} are equivalent ID of test microfin tubes and active cooling length 150 mm, respectively. $Q_{\mathrm{H2O,TS}}$, $Q_{\mathrm{gain,TS}}$, Q_{cond} are total heat transfer rate that cooling water gains, heat gain or leak from/to the ambient, and calculated conduction heat in the tube from outside of the active cooling length. The tube wall temperature at equivalent inner diameter $T_{\mathrm{wi,eq}}$ is corrected from the measured value T_{meas} by ϕ 0.127 mm thermocouples with one dimensional heat conduction through the tin layer and the microfin tube.

$$T_{\mathrm{wi,\,eq}} = T_{\mathrm{meas}} + \frac{Q_{\mathrm{TS}}}{2\pi\Delta Z_{\alpha}}\left[\frac{1}{\lambda_{\mathrm{tube}}}\ln\left(\frac{d_{\mathrm{wo}}}{d_{\mathrm{eq}}}\right) + \frac{1}{\lambda_{\mathrm{solder}}}\ln\left(\frac{d_{\mathrm{wo}} + 2\times 0.127\times 10^{-3}}{d_{\mathrm{wo}}}\right)\right] \quad (12)$$

where, λ_{tube} and $\lambda_{\mathrm{solder}}$ are thermal conductivities of tube material (copper) and solder. The overall HTC at the equivalent inner diameter of the test microfin tubes is,

$$\alpha = q_{\mathrm{wi,\,eq}}/\left(T_{\mathrm{b}} - T_{\mathrm{wi,\,eq}}\right) \quad (13)$$

4. RESULTS AND DISCUSSION

4.1 Assessment of Experimental Results and Predicting Correlations

Figure 4 shows experimental results of the comparative smooth and the test microfin tubes for CO_2 at a pressure of 6 MPa, mass flux of 100 kg $m^{-2}s^{-1}$, and heat flux of 10 kW m^{-2}. Refrigerant temperature at the test section inlet and outlet: $T_{\mathrm{b,i}}$ and $T_{\mathrm{b,o}}$, and the tube wall temperature: $T_{\mathrm{wi,eq}}$ are shown in the upper graphs. HTC are shown in the bottom graphs. The range of thermodynamic vapor quality x_{b} beyond 1 means superheat zone, where the bulk refrigerant temperature is above saturation point. In the graphs, symbols show experimental data with bars showing propagated measurement uncertainties for each value while lines show selected predicting correlations.

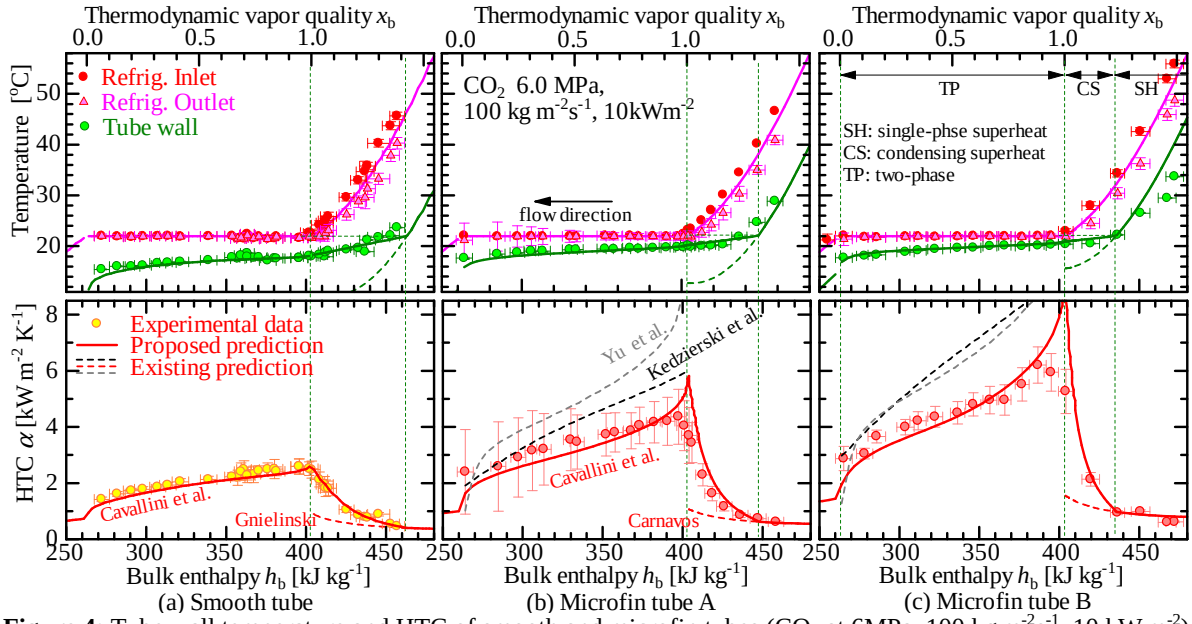

Figure 4: Tube wall temperature and HTC of smooth and microfin tubes (CO_2 at 6MPa, 100 kg $m^{-2}s^{-1}$, 10 kW m^{-2})

Table 2: Assessment of the experimental data and correlations proposed for microfin tubes

	Test Condition (Data points: TP/SH)	CO_2 in MicrofinA (228 / 71)		CO_2 in MicrofinB (28 / 12)		R410A in MicrofinA (179 / 16)	
		Ave. bias $\bar{\varepsilon}$	Standard devi. σ	Ave. bias $\bar{\varepsilon}$	Standard devi. σ	Ave. bias $\bar{\varepsilon}$	Standard devi. σ
TP	Cavallini et al. (2009)*' **	0.34	0.34	0.14	0.13	0.42	0.43
	Kedzierski and Goncalves (1997)*	0.42	0.41	0.37	0.18	0.41	0.37
	Yu and Koyama (1998)*	1.11	0.97	0.74	0.79	0.75	0.55
SH	Carnavos (1980)	0.02	0.29	0.04	0.21	-0.21	0.08
	Jensen and Vlakancic (1999)	-0.03	0.20	-0.21	0.13	-0.23	0.08
	Goto et al. (2005)	0.19	0.25	-0.11	0.19	0.02	0.11
	Ravigururajan and Bergles (1996)	0.62	0.41	0.53	0.23	0.22	0.12

* Liquid properties are evaluated at the film temperature. ** Using measured surface enlargement but not estimated value by trapezoidal rule

For the smooth tube, experimental HTC agrees well with correlations of Cavallini et al. (2006) modified by liquid properties evaluated at the film temperature (2012) in two-phase zone (TP) and Gnielinski (1976) in single-phase superheat zone (SH), respectively. Between single-phase and two-phase zones, where the bulk refrigerant temperature is above saturation but the tube wall temperature is below saturation, those two correlations should be invalid according to the heat transfer model. In this zone categorized as condensing superheat zone (CS), Equation (9) seamlessly connects from the correlation of Gnielinski (1970) to the correlation of Cavallini et al. (2006).

Table 2 compares the experimental data and predicting correlations for microfin tubes. Three correlations are selected for two-phase zone (TP); four correlations are selected for single-phase superheat zone (SH), where the tube wall temperature is above saturation temperature. It should be noted that the correlations are transcribed to the HTC based on the equivalent smooth tube, and liquid properties are evaluated at the film temperature in accordance with the correction method of Fujii et al. (1996). Additionally, the measured surface enlargement ratio was applied but not geometrically calculated value, since the fin geometry of microfin tube B is out of trapezoidal rule and most of corners are rounded. Average bias $\bar{\varepsilon}$ and standard deviation σ in Table 2 are,

$$\bar{\varepsilon} = \frac{1}{n}\sum_{j=1}^{n}\varepsilon_j = \frac{1}{n}\sum_{j=1}^{n}\left[\left(\alpha_{\mathrm{cal},j} - \alpha_{\mathrm{exp},j}\right)/\alpha_{\mathrm{exp},j}\right] \tag{14}$$

$$\sigma = \sqrt{\frac{1}{n-1}\sum_{j=1}^{n}\left(\varepsilon_j - \bar{\varepsilon}\right)^2} \tag{15}$$

As compared above, the average bias is positive to all test conditions in two-phase zone (TP), which means experimental HTC is lower than those three correlations. Nevertheless, except very near the critical point, experimental HTC agrees with correlations of Cavallini et al. (2009) within 30% roughly. Experimental HTC and correlations by Carnavos (1980), Jensen and Vlakancic (1999), and Goto et al. (2005) agree reasonably in single-phase superheat zone (SH), although those correlations are not validated at such high reduced pressures.

4.2 Effect of Microfin on HTC near the Critical Point

As divided by dashed vertical line in Figure 4, experimental HTC starts deviating from the correlations of single-phase zone at enthalpies 450, and 435 kJ kg^{-1} in microfin tube A and B, respectively. Those are corresponding to the point where the tube wall temperatures reach saturation point. This is exactly the same criterion of condensation occurrence as smooth tube, and the deviating HTC identifies this. By microfin A and B, HTC of single-phase superheat zone increase roughly 50% and 110% from the smooth tube for CO_2 at a pressure of 6MPa, mass flux of 100 kg $m^{-2}s^{-1}$, and heat flux 10 kW m^{-2}. The temperatures of microfin tubes are higher than that of the smooth tube and reach the saturation point at lower enthalpies. Thus, condensation starts at lower enthalpies. The maximum HTC of the microfin tubes A and B at thermodynamic vapor quality 1 are approximately 180% and 210% of the smooth tube. These increments correspond to the surface enlargement, as listed in Table 1. This suggests that the increase in heat transfer enlargement is one of the most contributing factors on heat transfer enhancement in the test microfin tubes.

Figure 5 shows change in HTC of the smooth and microfin tubes with increasing pressure across the critical points Symbols are experimental HTC; lines are predicted HTC calculated by Cavallini's correlation (2006, 2009) modified by the authors to include film temperature (Kondou and Hrnjak, 2012). Toward the critical point, HTC

decreases at the test conditions in consequence of compensating negative factors (e.g., decrease in liquid density, liquid thermal conductivity, latent heat, and vapor velocity), and positive factors (e.g., increase in specific heat). Then, HTC suddenly increases from reduced pressure 0.96 approximately as if elevated by suddenly increasing thermal conductivities and heat capacities of both phase. This drastic change in HTC is common to the smooth and test microfin tubes for both refrigerant CO_2 and R410A. Despite of such drastically changing refrigerant properties, the helical microfins appear to be almost constantly beneficial at the entire pressure range.

4.3 Proposal of the Predicting Method for Condensing Superheat Zone in Microfin Tubes

As described in Equation (9), the heat transfer coefficient forced by "bulk-to-wall" temperature difference in condensing superheat zone can be divided to heat transfer coefficient of de-superheating α_{SH} by "bulk-to-saturation" and saturated condensation α_{TP} by "saturation-to-wall" temperature difference. For smooth tubes, this predicting method was already demonstrated with the correlations of Gnielinski (1976) and Cavallini (2006), as shown by a solid line in Figure 4 (a). For microfin tubes, in consideration of the assessment of Table 2, it is speculated that those coefficients are given by correlations of Carnavos (1980) and Cavallini et al. (2009) associated with the modification using the film temperature. The predicted HTC is shown by red solid lines in Figures 4 (b) and (c). With high degree of overlapped of the solid lines and symbols, the proposed method Equation (9) is validated also for microfin tubes. The improvement is explicit in tube wall temperature as shown with green solid lines. As compared to the dashed and solid green lines, unnatural discontinuity of tube wall temperature in typical modeling approach is seamlessly connected from single-phase to two-phase zone by the proposed method.

Figure 6 compares the experimental and predicted HTC of the microfin tube A at various heat fluxes. In contrast to the predicted HTC, experimental HTC decreases with increasing heat flux in two-phase zone. Although this

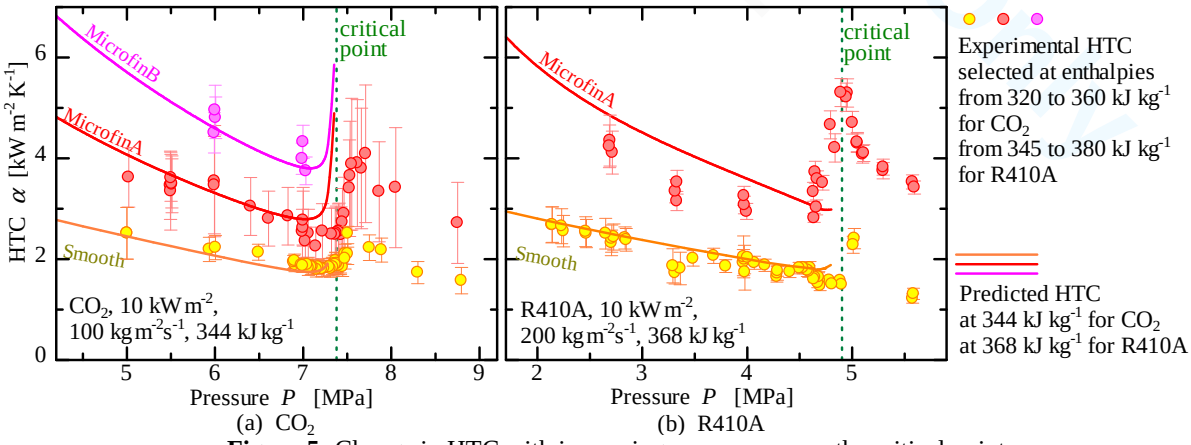

Figure 5: Change in HTC with increasing pressure across the critical point

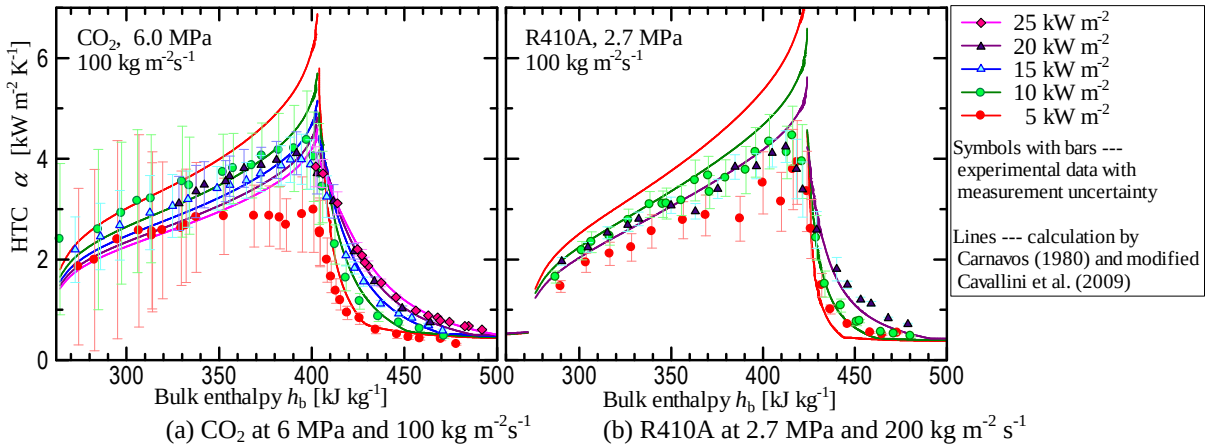

(a) CO_2 at 6 MPa and 100 kg $m^{-2}s^{-1}$ (b) R410A at 2.7 MPa and 200 kg m^{-2} s^{-1}

Figure 6: Effect of heat flux on the start point of condensation in the microfin tube A

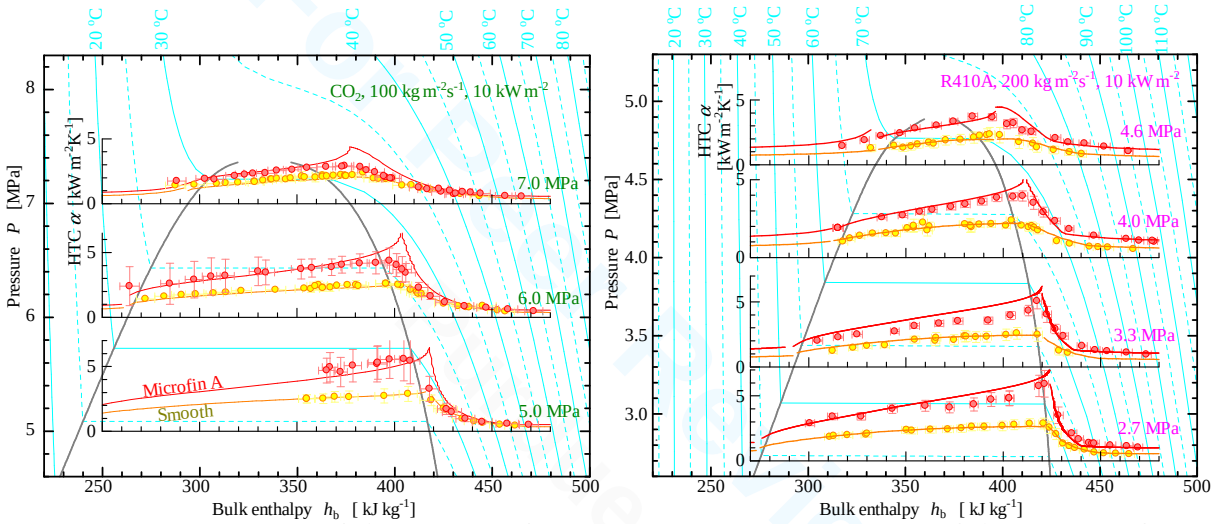

(a) CO_2 at 100 kg $m^{-2}s^{-1}$ and 10 kW m^{-2} (b) R410A at 200 kg $m^{-2}s^{-1}$ and 10 kW m^{-2}

Figure 7: Summary of HTC from superheat to two-phase zone in smooth and microfin tubes

discrepancy is not negligible at 5 kW m^{-2}, both HTC asymptotically plateau to the same value at heat fluxes above 10 kW m^{-2}. With increasing heat flux, the start point of condensation shifts to higher enthalpies. This is because the tube wall temperature tends to be lower at higher heat fluxes and reaches saturation point at higher enthalpies. Likewise, condensing superheat zone is strongly depends on the heat flux. As shown in Figure 6, the proposed method well predicts the changing condensation start point at various heat fluxes.

4.4 Effect of Condensing Superheat Zone on Condenser Designing

Figure 7 summarizes HTC of CO_2 and R410A from the single-phase superheat zone to the two-phase zone. HTC of smooth and microfin tube A at various pressures are plotted on the *P-h* diagrams for the purpose of showing the portion of the condensing superheat zone in total enthalpy changes through condensers. Symbols are the experimental HTC; lines are the proposed prediction Equation (9). Figure7 suggests that to consider the condensation occurrence in superheat zone into the entire heat rejection process becomes more important for condenser designing as approaching the critical point.

Figure 8 shows the case study on air-cooled cross-fin-tube type condensers using the microfin tube A for R410A at 2.7 MPa, where the typical operating condition of air conditioners in summer seasons. Air temperature is assumed uniformly 35 °C. Other air side parameters are assumed as noted on right side of the graphs. The calculated refrigerant temperature, the tube wall temperature, the heat flux at the equivalent inner diameter of microfin tube A, and the refrigerant side HTC are plotted from right side to left side along one circuit. The existing prediction is shown with dashed lines; the proposed prediction considering condensing the superheat zone is shown with solid lines. Under the graphs, the length of each zones calculated by the proposed and existing predictions are shown. According to the proposed prediction, condensation occurs in 70% of superheat zone. As shown in the circular graphs, in the superheat zone, the heat resistance of refrigerant side is 63% of total. This is roughly three times larger than well-known conditions of two-phase zone, which means refrigerant side performance affects condenser sizing more in this zone. In consequence of the condensation in presence of superheated vapor, the required tube length for completing two-phase condensation can be approximately 6% shorter even at the reduced pressure 0.55.

6. CONCLUSIONS

Heat rejection heat transfer coefficient data of flowing CO_2 and R410A from superheat to two-phase zone in horizontal microfin tubes has been experimentally investigated. The main findings are following:

- In the superheat zone, experimental heat transfer coefficient starts gradually deviating from the correlation proposed for single-phase cooling from when tube wall reaches saturation point. This identifies condensation occurrence in presence of superheated vapor at exactly same criteria as smooth tubes.

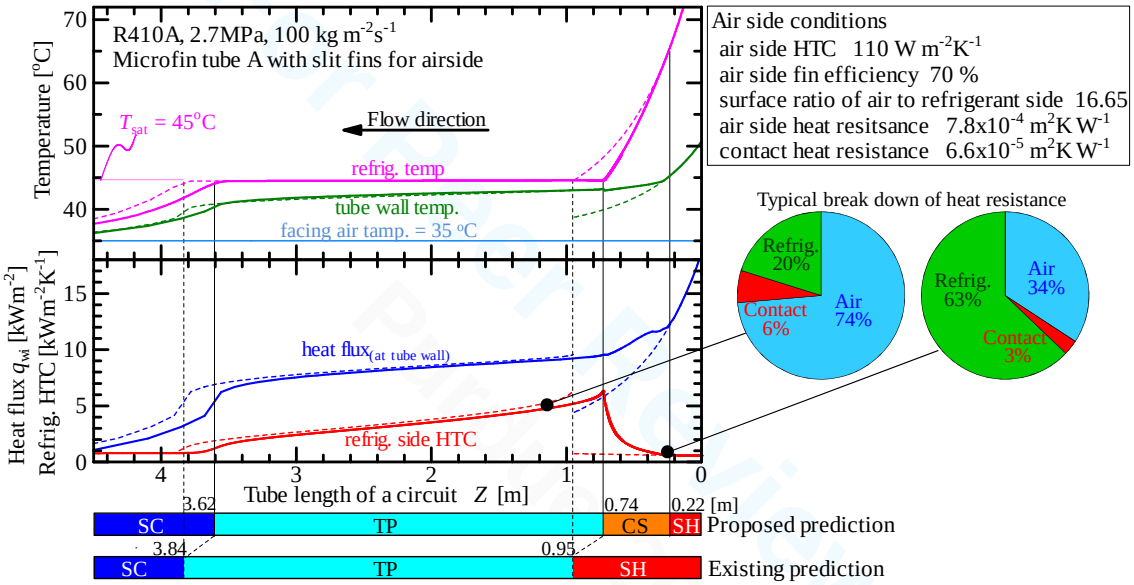

Figure 8: Case study for cross-fin-tube HEXs using R410A at 2.7 MPa

- A predicting correlation considering condensation superheated vapor was derived from a heat balance in superheated vapor and coexisting condensate.
- The predicting correlation, which combines two correlations of Carnavos (1980) and Cavallini et al. (2009) evaluates the liquid properties at film temperature, was validated with experimental results at the reduced pressure ranging from 0.55 to 0.95.
- Condensing occurrence in superheat zone affects condenser sizing. This was demonstrated with the case study of typical cross-fin-tube heat exchanger using microfin tubes for R410A at 2.7 MPa.
- To consider the condensation occurrence in superheat zone becomes more important for condenser designing as approaching the critical point, because the degree of superheat at compressor discharge becomes higher and the latent heat becomes smaller.

NOMENCLATURE

Cp	specific heat	(J kg^{-1} K^{-1})	**Subscripts**	
d	diameter	(m)	b	bulk refrigerant
h	specific enthalpy	(J kg^{-1})	cal	calculated
$\dot{m}$	mass flow rate	(kg s^{-1})	cond	conduction heat
n	number of data	(-)	eq	equivalent inner diameter
N_{fin}	number of fins	(-)	exp	experimental
P	pressure	(Pa)	gain	heat gain or leak
q	heat flux	(W m^{-2})	H2O	water
Q	heat transfer rate	(W)	i	inlet
T	temperature	(^{o}C)	L	liquid
x_a	actual vapor quality	(-)	latent	latent
x_b	thermodynamic vapor quality	(-)	max	maximum or nominal
Z	tube length	(m)	meas	measured
α	heat transfer coefficient	(W m^{-2}K^{-1})	mixer	mixer
β	lead angle of microfin	(^{o})	o	outlet
δ_{fin}	height of microfin	(m)	PC	pre-cooler
Δh	enthalpy change	(J kg^{-1})	sat	Saturated
Δh_{LV}	vaporization latent heat	(Pa)	SC	Subcool
ΔP	pressure drop	(m)	SH	Superheat
ΔZ_{α}	active cooling length	(-)	total	Total

ε	relative deviation	(-)	TP	two-phase
$\bar{\varepsilon}$	average bias	(^{o})	TS	test section
γ	apex angle of microfin	(-)	V	Vapor
η_A	surface enlargement ratio	(W m^{-1})	wi	internal tube wall
λ	thermal conductivity	(-)	wo	outer tube wall
σ	standard deviation	(J kg^{-1})		

REFERENCES

Altman, M., Staub, F.W., Norris, R.H., 1959, Local Heat Transfer and Pressure Drop for Refrigerant-22 Condensing in Horizontal tubes, *Chem. Eng. Prog. Symposium Series*. vol. 56, no. 30: p. 151-159.

Bell, K.J., 1972, Temperature Profiles in Condensers, *Chem. Eng. Prog.*, vol. 68, no. 7: p. 81-82.

Carnavos, T.C., 1980, Heat Transfer Performance of Internally Finned Tubes in Turbulent Flow, *Heat Transfer Eng.*, vol. 1, no. 4: p. 32-37.

Cavallini, A., Del Col, D., Doretti, L., Matkovic, M., Rossetto, L., Zilio, C., Censi, G., 2006, Condensation in Horizontal Smooth Tubes: a new heat transfer model for heat exchanger design, *Heat Transfer Eng.*, vol. 27, no. 8: p. 31-38.

Cavallini, A., Del Col, D., Mancin, S., Rossetto, L., 2009, Condensation of Pure and Near-Azeotropic Refrigerants in Microfin Tubes: a new computational procedure, *Int. J. Refrig.*, vol. 32: p. 162-174.

Fujii, T., Honda, H., Nozu, S., Nakarai, S., 1978, Condensation of Superheated Vapor Inside a Horizontal Tube, *Heat Transfer - Japanese Research*, vol. 4, no. 3: p. 1-48.

Fujii, T., Lee, J.B., Shinzato, K., 1996, Laminar Forced Convection of Saturated Vapors in the Near-Critical Region, *Int. J. Numer. Heat Transfer, Part A*, vol. 30: p. 799-813.

Gnielinski, V., 1976, New Equation of Heat and Mass Transfer in Turbulent Pipe and Channel Flow. *Int. Chem. Eng.*, vol. 16: p. 359-367.

Goto, M., Inoue, M., Shiromoto, K., Emoto, Y., Li, Y., Sato, M., Kiyotani, A., 2005, Development of General Correlation for Heat transfer in Single-Phase Turbulent Flow Inside Internally Helical-Grooved Tubes. *Trans. JSRAE*, vol. 22, no. 4: p. 437 - 447 (in Japanese).

Jensen, M.K., Vlakancic, A., 1999, Experimental Investigation of Turbulent Heat Transfer and Fluid Flow in Internally Finned Tubes, *Int. J. Heat Mass Transfer*, vol. 42: p. 1343-1351.

Kedzierski, M.A., Goncalves, J.M., 1997, Horizontal Convective Condensation of Alternative Refrigerants within a Mifro-Fin Tube, *NIST IR6095*, National Institute of Standards and Technology, Gaithersburg, Maryland: p. 1-74.

Kondou, C., Hrnjak, P.S., 2012, Condensation from Superheated Vapor Flow of R744 and R410A at Subcritical Pressures in a Horizontal Smooth Tube", *Int. J. Heat Mass Transfer*, vol. 55: p. 2779–2791

Lee, C.C., Teng, Y.J., Lu, D.C., 1991, Investigation of Condensation Heat Transfer of Superheated R-22 Vapor in a Horizontal tube, *Proc. World Conf. Exp. Heat Trans. Fluid Mech. and Thermodynamics*: p. 1051-1057.

Lemmon, E.W., Huber, M.L., McLinden, M.O., 2007, *Reference Fluid Thermodynamic and Transport Properties - REFPROP ver.8.0*, National Institute of Standards and Technology, Boulder, CO, USA.

Ravigururajan, T.S., Bergles, A.E., 1996, Development and Verification of General Correlations of Pressure Drop and Heat Transfer in Single-Phase Turbulent Flow in Enhanced Tubes, *Exp. Therm. Fluid Sci.*, vol. 13: p. 55-70.

Webb, R.L., 1998, Convective Condensation of Superheated Vapor, *Trans. ASME, J. Heat Transfer*, vol. 120: p. 418-421.

Yu, J., Koyama, S., 1998, Condensation Heat Transfer of Pure Refrigerants in Microfin Tubes, *Proc. Int. Refrig. Conf. at Purdue*: p. 325-330.

ACKNOWLEDGEMENT

The authors are deeply grateful for financial support from the Air Conditioning and Refrigeration Center (ACRC) of the University of Illinois, technical support (instrumentation and original experimental facility) from Creative Thermal Solutions, Inc. (CTS), and microfin tubes kindly donated by Wieland-Werke AG.